Electronic Absorption and Fluorescence Spectra of [2.2]Anthracenophanes

Masaharu MORITA,† Tohru KISHI,†† Masashi TANAKA, Jiro TANAKA,*
James FERGUSON,** Yoshiteru SAKATA,*** Soichi MISUMI,***
Toyoharu HAYASHI,**** and Noboru MATAGA****

Department of Chemistry, Faculty of Science, Nagoya University, Chikusa, Nagoya, 464
***Research School of Chemistry, Australian National University, Canberra, A.C.T. 2600 Australia*
****The Institute of Scientific and Industrial Research, Osaka University, Suita, Osaka, 565*
*****Department of Chemistry, Faculty of Engineering Science, Osaka University, Toyonaka, Osaka, 560*

(Received May 4, 1978)

The absorption and the fluorescence spectra of four [2.2]anthracenophanes were investigated at low temperatures. A theoretical calculation of the energy levels was performed by including the charge resonance and the exciton type interactions. The fluorescence excitation polarization spectra were recorded for all absorption bands at low temperatures, the directions of the transition moment of the excimer type emission bands being estimated by the *p*-values and the established transition directions of anthracene chromophores. The assignments of the absorption bands are presented based on these results.

The sandwich dimer is formed by photocleavage of dianthracene in rigid glass at low temperatures. Chandross *et al.*[1] and Ferguson *et al.*[2] found that the dimer shows excimer type emission at low temperatures but the absorption spectra slightly differ from a monomer spectrum and are correlated by a weak coupling vibronic theory. Ferguson and Mau[3] found the absorption of the anthracene sandwich pairs in dianthracene crystal.[3] In studies on the emission spectra of 9,10-dichloroanthracene crystal, Tanaka and Shibata[4] found that only the β crystalline form emits an excimer type emission, suggesting that a favorable geometrical arrangement of molecules in the crystal is necessary for formation of the excimer.

As a next step it is important to study the dimer interaction with a rigid molecule, *viz.*, anthracenophanes. Anthracenophanes have two anthracene chromophores separated by two ethylene bridges with a fixed or limited motion of composite rings; thus the inter-ring interaction should be more precisely investigated. Recently accurate X-ray crystal structure analyses of two anthracenophanes were carried out, the geometry and interatomic distances of these molecules being determined.[5,6] We have investigated the absorption and fluorescence spectra of four anthracenophanes at room temperature and low temperatures, and recorded the polarization of the fluorescence excitation spectra. A part of the emission work was published.[7] A theoretical calculation of the excited levels of these molecules was performed, and the assignments of the spectra are presented. It has been shown that the exciton type and the charge resonance type interactions between two chromophores are very important in molecules of close ring contact.[8-10] The structure of the excimer of anthracene is discussed from the reslults of the absorption and emission spectra of anthracenophanes.

† Former Research Fellow of Research School of Chemistry, Australian National University.
Present address: Matsumoto Dental College, Shiojiri, Nagano
†† Visiting researcher from The Institute of Police Science, Tokyo.

Experimental

The materials were synthesized by the methods reported.[11,12] The shape and name of molecules are shown in Fig. 1. The solvent 2-methyltetrahydrofuran of spectrograde was distilled with sodium metal after treatment with potassium hydroxide.

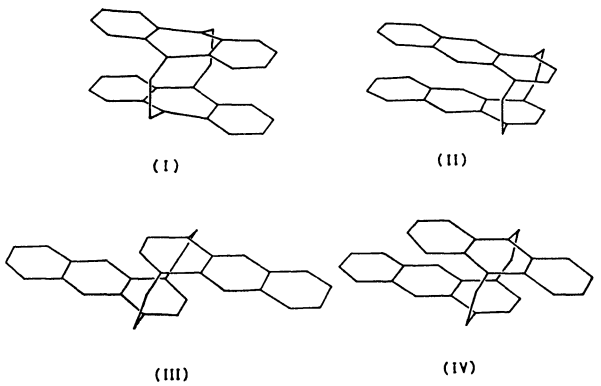

Fig. 1. [2.2]Anthracenophanes: (I) [2.2](9,10)anthracenophane; (II) *syn*-[2.2](1,4)anthracenophane; (III) *anti*-[2.2](1,4)anthracenophane; (IV) [2.2](1,4)(9,10)-anthracenophane.

The absorption spectra were recorded with a Cary 15 spectrophotometer with a Cryo-tip refrigerator for the low temperature measurement. A Cary 17 spectrophotometer at Australian National University was also used with a flow type cryostat. The fluorescence spectra were measured on a Carl-Zeiss M4QIII spectrofluorometer with a HTV R446 photomultiplier tube. The sample was excited with a 1 kW Xe lamp through a Carl-Zeiss monochromator set at right angles to the entrance slit of the fluorometer. Measurements of emission were also made with a 3/4 m Spex spectrometer, a cooled ITT-FW130 photomultiplier being used. The light from a 150W Varian xenon illuminator dispersed by a Carl-Zeiss MM 12 double monochromator was used as exciting source.[2,3] The intensity of fluorescence was corrected by comparison with that of quinine bisulfate solution in 0.1 N H_2SO_4 and of *o*-dichlorobenzene solution of 4-dimethylamino-4′-nitrostilbene. The polarization of the emission (PF) and the excitation (APF) was measured with the same system combined with calcite and pola-coat polarizers, the polarization character of the system

being cheked beforehand. The lifetime of the emission band was measured with a pulsed nitrogen gas laser combined with a Tektronix synchroscope of 465 type or a Tektronix sampling scope 564-3S2-3T77A system. The NMR spectra were recorded on JEOL JNM-TS-100 at 23, −50, −95, and −100 °C.

Theoretical Calculation

A SCF MO of each anthracene chromophore was calculated by the P-P-P method[13,14] with Nishimoto-Mataga potential.[15] The calculation was based on the structures determined by X-ray crystal analysis.[5,6] For molecules whose structures have not been determined by the X-ray method, model structures were constructed from the known forms.

The ground state wavefunctions of each ring are written as follows.

$$\begin{aligned} \Phi_0 &= |\varphi_1\bar{\varphi}_1 \cdots \varphi_7\bar{\varphi}_7| \\ \Theta_0 &= |\theta_1\bar{\theta}_1 \cdots \theta_7\bar{\theta}_7| \end{aligned} \tag{1}$$

The energies of the excited states were calculated from configuration interactions, where the intergroup charge resonance (CR) and the exciton interactions are included. The matrix elements between the locally excited (LE) and CR states were calculated by using the following formulas.

$$\begin{aligned} &\langle\varphi_m\varphi_n|H|\varphi_m\theta_n\rangle \\ &\quad= \frac{1}{2}\langle\{|\cdots\varphi_m\bar{\varphi}_n\cdots|+|\cdots\varphi_n\bar{\varphi}_m\cdots|\} \\ &\qquad||H||\{|\cdots\varphi_m\bar{\theta}_n\cdots|+|\cdots\bar{\theta}_n\varphi_m\cdots|\}\rangle \\ &\quad= \langle\varphi_n|F|\theta_n\rangle + 2(\varphi_m\theta_n|\varphi_m\varphi_n) - (\varphi_m\varphi_m|\varphi_n\theta_n), \\ &\langle\varphi_m\varphi_n|H|\theta_m\varphi_n\rangle \\ &\quad= \frac{1}{2}\langle\{|\cdots\varphi_m\bar{\varphi}_n\cdots|+|\cdots\varphi_n\bar{\varphi}_m\cdots|\} \\ &\qquad||H||\{|\cdots\theta_m\bar{\varphi}_n\cdots|+|\cdots\varphi_n\bar{\theta}_m\cdots|\}\rangle \\ &\quad= -\langle\varphi_m|F|\theta_m\rangle + 2(\varphi_m\varphi_n|\theta_m\varphi_n) - (\varphi_m\theta_m|\varphi_n\varphi_n), \end{aligned} \tag{2}$$

where Coulomb hybrid integrals are denoted by

$$(\varphi_m\theta_m|\varphi_n\varphi_n) = \int\varphi_m(1)\theta_m(1)\frac{1}{r_{12}}\varphi_n(2)\varphi_n(2)dv_1dv_2.$$

The hybrid integrals are calculated by using Mulliken's approximation

$$(\varphi_m\theta_m|\varphi_n\varphi_n) = \frac{1}{2}S_{mm}\{(\varphi_m\varphi_m|\varphi_n\varphi_n)+(\varphi_n\varphi_n|\theta_m\theta_m)\},$$

$$S_{mm} = \langle\varphi_m|\theta_m\rangle = \int\varphi_m(1)\theta_m(1)dv_1.$$

The one-electron integrals extending over two rings are taken as proportional to the overlap integrals:

$$\langle\varphi_n|F|\theta_n\rangle = kS_{nn}. \tag{4}$$

The proportionality constant, k, was so chosen as to obtain the best fit of calculated results with the observed values of transition energies and set to −14.0 eV. All computations were carried out on a Facom 230-60 computer at Nagoya University Computation Center.

Feature of Anthracenophane Excited State. Anthracene monomers have three excited states in the 25000—48000 cm^{-1} region, two of which are observed as allowed transitions. The lower energy transition in the 25000 cm^{-1} region is the short-axis polarized band ($^1B_{2u}$ state, ^1L_a band). It is composed of the electronic excitation from the highest occupied MO (φ_7, HOMO) to the lowest unoccupied MO (φ_8, LUMO). We can abbreviate the wavefunction of this state to

$$\Phi_1 = \frac{1}{\sqrt{2}}\{|\cdots\varphi_7\bar{\varphi}_8|+|\cdots\varphi_8\bar{\varphi}_7|\}. \tag{5}$$

The higher and stronger absorption is the long-axis polarized transition to the $^1B_{3u}$ state (^1B_b band); the wavefunction of the state is described by a linear combination of the excitation of an electron from the second HOMO (φ_6) to the LUMO (φ_8) and from the HOMO (φ_7) to the second LUMO (φ^9) as

$$\begin{aligned} \Phi_2 = \frac{1}{2}\{&|\cdots\varphi_6\bar{\varphi}_8\cdots|+|\cdots\varphi_8\bar{\varphi}_6\cdots| \\ &+|\cdots\varphi_7\bar{\varphi}_9|+|\cdots\varphi_9\bar{\varphi}_7|\}. \end{aligned} \tag{6}$$

A forbidden transition (^1L_b band) is composed of antisymmetric combination of the same excitation orbitals and is expected in the region of the first band, however, it has never been observed in the anthracene molecule.

When two anthracenophane chromophores approach each other, the CR configuration and the exciton type interaction become significant. The wavefunction of the exciton type state of the short-axis polarized first band is written as

$$\begin{aligned} ER_1(+) &= \frac{1}{\sqrt{2}}\{\Phi_1\Theta_0+\Phi_0\Theta_1\}, \\ ER_1(-) &= \frac{1}{\sqrt{2}}\{\Phi_1\Theta_0-\Phi_0\Theta_1\}. \end{aligned} \tag{7}$$

If the two chromophores are related by an inversion symmetry, the $ER_1(+)$ state is forbidden and the $ER_1(-)$ state allowed.

The CR configuration of the same symmetry type are given by

$$\begin{aligned} CR_1(+) &= \frac{1}{\sqrt{2}}\{\Phi_1^+\Theta_1^-+\Phi_1^-\Theta_1^+\} \\ \text{and} \\ CR_1(-) &= \frac{1}{\sqrt{2}}\{\Phi_1^+\Theta_1^--\Phi_1^-\Theta_1^+\}. \end{aligned} \tag{8}$$

The energies of these configurations may be nearly degenerate, and the configuration interaction between the same symmetry levels should be considered. The resultant states can be approximately written as

$$\begin{aligned} \text{forbidden states} &\begin{cases} ER_1(+) + CR_1(+) \\ ER_1(+) - CR_1(+) \end{cases} \\ \text{allowed states} &\begin{cases} ER_1(-) + CR_1(-) \\ ER_1(-) - CR_1(-). \end{cases} \end{aligned} \tag{9}$$

The exciton states of the long-axis polarized transition are given by a linear combination of each LE state as

$$\begin{aligned} ER_2(+) &= \frac{1}{\sqrt{2}}(\Phi_2\Theta_0+\Phi_0\Theta_2), \\ ER_2(-) &= \frac{1}{\sqrt{2}}(\Phi_2\Theta_0-\Phi_0\Theta_2). \end{aligned} \tag{10}$$

The charge resonance excited levels of the same orbital type are written as $\Phi_2^+\Theta_2^-$. They are combined to give two CR states as

Table 1. Calculated and observed energy levels of [2.2](9,10)anthracenophane

	State	Energy (cm^{-1}) Calcd (Obsd)	Intensity (f) Calcd (Obsd)	Wave function
1	Ground	0		$0.98\Phi_0\Theta_0+0.10\phi_6\theta_8+0.11\theta_6\phi_8-0.08\theta_7\phi_9+0.07\phi_7\theta_9$
2	$ER_1(+)+CR_1(+)$	17950 (19000)	0.0002 (0.002)	$0.50\phi_7\phi_8+0.46\theta_7\theta_8+0.47\phi_7\theta_8+0.49\theta_7\phi_8$
3	$ER_1(-)+CR_1(-)$	25250 (24000)	0.008 (0.03)	$0.16\phi_7\phi_8-0.18\theta_7\theta_8+0.62\phi_7\theta_8-0.59\theta_7\phi_8$
4	$ER_1(-)-CR_1(-)$	28060 (26247)	0.19 (0.05)	$0.51\phi_7\phi_8-0.65\theta_7\theta_8-0.25\phi_7\theta_8+0.21\theta_7\phi_8$
5	$ER_2(+)+CR_2(+)$	29800 (31300)	0.002 (0.01)	$0.49\phi_7\phi_9+0.45\theta_7\theta_8+0.23\phi_6\phi_8+0.27\theta_6\theta_8+0.34\phi_7\theta_9+0.34\theta_7\phi_9+0.26\phi_6\theta_8+0.27\theta_6\phi_8$
6	$CR_2(-)$	34757 (34000)	0.09 (0.03)	$0.33\phi_7\theta_9-0.31\theta_7\phi_9-0.44\phi_6\theta_8+0.40\theta_6\phi_8$
7	$CR_2'(-)$	36660 (35600)	0.08 (0.16)	$0.53\phi_7\theta_9-0.46\theta_7\phi_9+0.40\phi_6\theta_8-0.45\theta_6\phi_8$
8	$ER_2(-)-CR_2(-)$	39620 } (39000)	0.87 } (0.86)	$0.29\phi_7\phi_9-0.29\theta_7\theta_9+0.28\phi_6\phi_8-0.32\theta_6\theta_8-0.16\phi_7\theta_9+0.17\theta_7\phi_9+0.16\phi_6\theta_8-0.08\theta_6\phi_8+0.35\phi_6\phi_{10}-0.26\theta_6\theta_{10}-0.30\phi_5\phi_9+0.20\theta_5\theta_9$
9	$ER_2(-)+CR_2(-)$	41400	1.10	$0.48\phi_7\phi_9-0.18\theta_7\theta_9+0.27\phi_6\phi_8-0.37\theta_6\theta_8-0.03\phi_7\theta_9-0.43\theta_7\phi_9-0.07\phi_6\theta_8+0.33\theta_6\phi_8$

Table 2. Calculated and observed energy levels of *syn*-[2.2](1,4)anthracenophane

	State	Energy (cm^{-1}) Calcd (Obsd)	Intensity (f) Calcd (Obsd)	Wave function
1	Ground	0		$0.98\Phi_0\Theta_0+0.14\phi_6\theta_8-0.08\theta_6\phi_8+0.11\phi_7\theta_9+0.05\theta_7\phi_9$
2	$ER_1(+)+CR_1(+)$	20250 (20500)	6×10^{-4}	$0.44\phi_7\phi_8+0.45\theta_7\theta_8+0.35\phi_7\theta_8+0.52\theta_7\phi_8$
3	Coupled $^1B_{3u}$	26030 (24500)	1.5×10^{-3} (0.01)	$0.49\phi_6\theta_8-0.40\theta_6\phi_8-0.40\phi_7\theta_8+0.32\theta_7\theta_9+0.23\phi_6\theta_8-0.32\theta_6\phi_8+0.20\phi_7\theta_8-0.16\theta_7\phi_8+0.14\phi_7\theta_9-0.21\theta_7\phi_9$
4	$CR_1(-)$	26980 (26300)	4.4×10^{-3}	$0.19\phi_7\phi_8+0.29\theta_7\theta_8+0.55\phi_7\theta_8-0.37\theta_7\phi_8-0.42\phi_5\theta_8-0.10\theta_5\theta_8-0.04\phi_5\theta_8-0.35\theta_5\phi_8$
5	$ER_1(-)$	28590 (26800)	0.18 (0.085)	$0.63\phi_7\phi_8-0.54\theta_7\theta_8+0.02\phi_7\theta_8+0.17\theta_7\phi_8-0.06\phi_5\phi_8+0.25\theta_5\theta_8-0.36\phi_5\theta_8-0.04\phi_5\phi_8$
6	$ER_2(-)+CR_2(-)$	31530 (33000)	0.027 (0.057)	$0.30\phi_7\phi_9+0.36\theta_7\theta_9-0.18\phi_7\theta_9-0.27\theta_8\phi_8-0.07\phi_7\phi_8-0.24\theta_7\theta_8+0.26\phi_6\phi_8-0.25\theta_6\theta_8+0.10\phi_6\theta_8+0.42\theta_6\phi_8$
7	Mixed higher ER+CR	36470 (37740)	0.12 (0.104)	$0.13\phi_7\phi_8+0.23\theta_7\theta_8-0.14\phi_7\theta_8-0.29\theta_7\phi_8+0.19\phi_7\theta_9+0.18\theta_7\phi_9-0.42\phi_6\theta_8-0.26\theta_6\phi_8+0.16\phi_5\theta_8+0.35\theta_5\phi_8+0.11\phi_5\phi_8-0.35\theta_5\theta_8$
8	$ER_2(-)-CR_2(-)$	42420 (40650)	1.62 (1.06)	$0.47\phi_7\phi_9-0.36\theta_7\theta_9-0.19\phi_7\theta_9+0.21\theta_7\phi_9+0.52\phi_6\phi_8-0.24\theta_6\theta_8-0.27\phi_6\theta_8-0.08\theta_6\phi_8-0.17\phi_6\phi_9+0.22\theta_6\theta_9$

Table 3. Calculated and observed energy levels of *anti*-[2.2](1,4)anthracenophane

	State	Energy (cm^{-1}) Calcd (Obsd)	Intensity (f) Calcd (Obsd)	Wave function
1	Ground	0		$0.99\Phi_0\Theta_0+0.10\phi_7\theta_9+0.10\theta_7\phi_9$
2	$ER_1(+)+CR_1(+)$	23200 (23900)	0.011 (0.009)	$0.47\phi_7\phi_8+0.16\theta_7\theta_8+0.58\phi_7\theta_8+0.20\theta_7\phi_8+0.15\phi_5\phi_8+0.26\theta_5\theta_8+0.31\phi_5\theta_8+0.22\theta_5\phi_8$
3	$ER_1(-)+CR_1(-)$	23300 (24750)	0.064 (0.08)	$0.23\phi_7\phi_8-0.51\theta_7\theta_8+0.29\phi_7\theta_8-0.62\theta_7\phi_8$
4	$ER_1(-)-CR_1(-)$	29623 (25250)	0.135 (0.06)	$0.52\phi_7\phi_8-0.44\theta_7\theta_8-0.21\phi_7\theta_8+0.17\theta_7\phi_8+0.18\phi_5\phi_8-0.14\theta_5\theta_8-0.33\phi_5\theta_8+0.30\theta_5\phi_8$
5	Higher CR	33130 (30000)	4×10^{-4} (0.02)	$0.29\phi_5\phi_8+0.36\theta_5\theta_8-0.39\phi_7\theta_8-0.42\theta_7\phi_8+0.33\phi_5\theta_8+0.23\theta_5\phi_8$
6	$ER_2(-)+CR_2(-)$	35100 } (35300)	0.59 } (1.30)	$0.24\phi_7\phi_9-0.27\theta_7\theta_9+0.11\phi_7\theta_9-0.11\theta_7\phi_9+0.16\phi_6\phi_8-0.18\theta_6\theta_8+0.50\phi_6\theta_8-0.52\theta_6\phi_8$
7	$ER_2(-)+CR'_2(-)$	37000	1.12	$0.22\phi_7\phi_9-0.25\theta_7\theta_9+0.33\phi_7\theta_9-0.35\theta_7\phi_9+0.36\phi_6\phi_8-0.38\theta_6\theta_8-0.08\phi_6\theta_8+0.09\theta_6\phi_8$
8	$ER_2(-)-CR_2(-)$	39200 (39500)	0.40 (1.00)	$0.25\phi_6\phi_8-0.22\theta_6\theta_8-0.31\phi_6\theta_8+0.31\theta_6\phi_8-0.42\phi_6\phi_{10}+0.41\theta_6\theta_{10}+0.29\phi_5\phi_9-0.28\theta_5\theta_9$

Table 4. Calculated and observed energy levels of [2.2](1,4)(9,10)anthracenophane

	State	Energy Calcd (Obsd)	Intensity (f) Calcd (Obsd)	Wave function
1	Ground	0		$0.99\Phi_0\Theta_0+0.07\phi_7\theta_9+0.08\theta_7\phi_9-0.05\phi_6\theta_8+0.09\theta_6\phi_8$
2	$ER_1(+)+CR_1(+)$	17160 (22500)	1×10^{-4} (0.002)	$0.41\phi_7\phi_8+0.41\theta_7\theta_8+0.51\phi_7\theta_8+0.34\theta_7\phi_8+0.10\phi_5\phi_8+0.35\theta_5\theta_8+0.12\phi_5\theta_8+0.25\theta_5\phi_8$
3	$ER_1(-)+CR_1(-)$	21850 (23800)	0.059 (0.077)	$0.18\phi_7\phi_8-0.54\theta_7\theta_8+0.45\phi_7\theta_8-0.56\theta_7\phi_8-0.17\phi_5\phi_8+0.27\theta_5\theta_8-0.12\phi_5\theta_8$
4	$ER_1(-)-CR_1(-)$	26920 (27600)	0.16 (0.10)	$0.56\phi_7\phi_8-0.47\theta_7\theta_8-0.22\phi_7\theta_8+0.32\phi_7\theta_8+0.10\phi_5\phi_8-0.21\theta_5\theta_8-0.12\phi_5\theta_8-0.31\theta_5\phi_8$
5	$ER_2(-)+CR_2(-)$	34440 (35500)	0.42 (0.87)	$0.22\phi_7\phi_9-0.28\theta_7\theta_9+0.35\phi_7\theta_9-0.29\theta_7\phi_9-0.19\theta_6\theta_8+0.54\phi_6\theta_8-0.45\theta_6\phi_8$
6	$ER_2(-)-CR_2(-)$	39620 (39000)	1.47 (1.15)	$0.32\phi_7\phi_9-0.46\theta_7\theta_9+0.39\theta_7\phi_9+0.33\phi_6\phi_8-0.48\theta_6\theta_8+0.27\theta_6\phi_8$

$$CR_2(+)=\frac{1}{\sqrt{2}}(\Phi_2^+\Theta_2^-+\Phi_2^-\Theta_2^+),$$
$$CR_2(-)=\frac{1}{\sqrt{2}}(\Phi_2^+\Theta_2^--\Phi_2^-\Theta_2^+). \quad (11)$$

Since the energy levels of the ER_2 and the CR_2 states do not differ a great deal, the same symmetry levels are coupled to give new states as given by Eq. 9.

The calculated results on the energy levels for each molecule are given in Tables 1—4. Only allowed transtions are compiled, assignments by abbreviated notations being given in the first column. The results show that the excited levels of anthracenophanes are described by a complex linear combination of LE and CT transitions of each anthracene chromophore. Actually the structure of the molecule deviates from an inversion symmetry, so that the calculated MO and the state functions lose symmetric properties. Lowering of molecular symmetry makes some transitions allowed, which were originally forbidden in anthracene molecule. Weak transitions appear as a result of the inter-chromophore interactions.

In spite of these complication the feature of anthracenophane absorption bands is characterized by the allowed states of Eq. 9 and allowed combinations of $ER_2(-)\pm CR_2(-)$. The excimer emission state is related to the lowest forbidden state of Eq. 9, which includes nearly a half $CR_1(+)$ state.

Results and Discussion

[2.2](9,10)Anthracenophane (I). The absorption spectra measured at room temperature and 77 K are shown in Fig. 2. A number of absorption peaks were found, at least six excited levels being discerned. The lowest energy transition was found in the range 19000—23000 cm^{-1} with weak intensity and broad band shape. Since the intensity is very weak and the level is much lower than other levels, the band is assigned to a forbidden transition to a mixed state of the $CR_1(+)$ and $ER_1(+)$. Murrell and Tanaka[8] represented this excited level as a mixed state of $^1E_g-{}^1R_g$, where ^1E_g and ^1R_g correspond to $ER_1(+)$ and $CR_1(+)$, respectively. In earlier studies on anthracene dimer or anthracene crystals, no such forbidden band had been observed in this region. Recently such transitions have been observed in bridged anthracene derivatives.[3] The

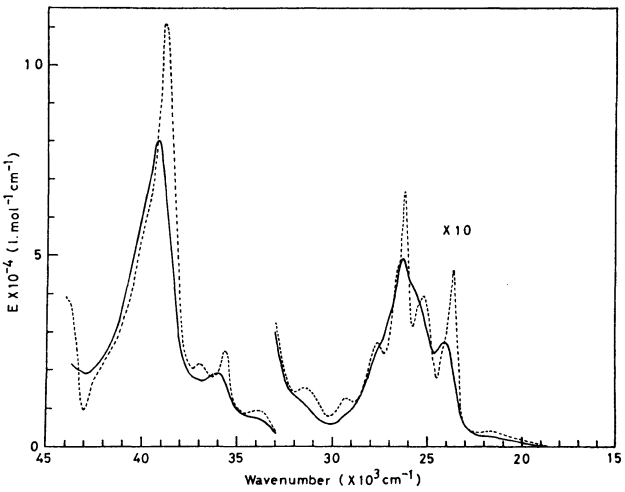

Fig. 2. Absorption spectra of I at 298 K (full line) and at 77 K (broken line) in MTHF.

inter-ring contact of this molecule is very close in the ground state, hence such type band is observed. The absorption band may be correlated with the excimer type emission of anthracene dimer, but the molecule gives no fluorescence even at 4 K. The absence of emission is ascribed to an efficient photochemical reaction and radiationless transitions.[7,16]

In the allowed transitions observed in the succeeding

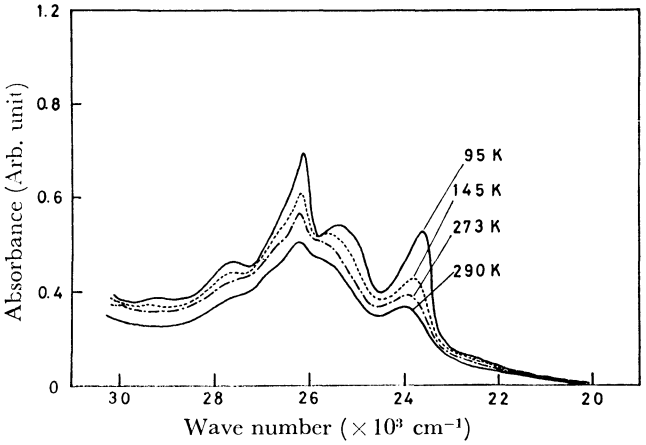

Fig. 3. Absorption spectra of I at various temperaures in MTHF.

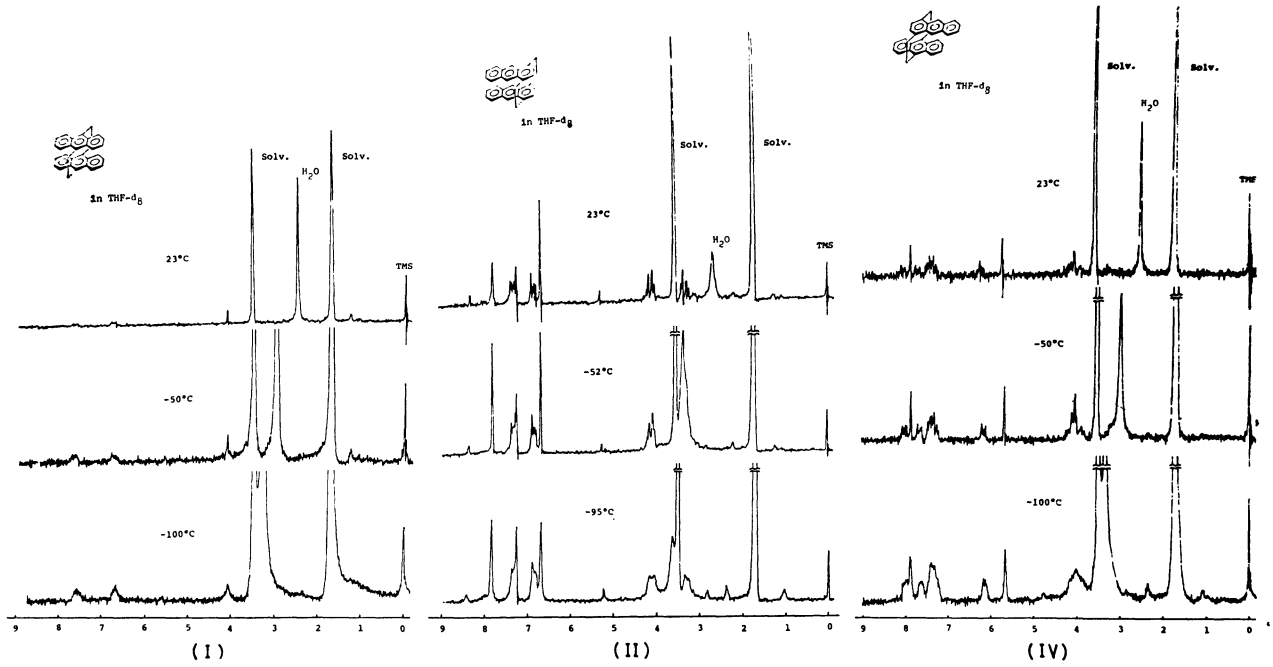

Fig. 4. NMR spectra of I, II, and IV at various temperatures.

region, the band at 24000 cm^{-1} is assigned to the transition of $ER_1(-)+CR_1(-)$. The next band at 25510 cm^{-1} shows strange spectral behavior with lowering in temperature; its intensity does not increase as compared to nearby transitions which are enhanced significantly. The intensity of this band is recorded as a guest in the single crystal of the photoisomer host, its intensity being much larger at 10 K as compared to that at 206 K.[17] The temperature change of solution spectra in this region shows that the 25510 cm^{-1} band behaves differently as compared to the neighboring bands (Fig. 3). Such unusual spectral behavior may be accounted for by assigning the band to the conformational isomer whose spectrum differs from that of the major conformer in this region.[18] The X-ray data on *syn*-[2.2](1,4)anthracenophane show the presence of two conformational isomers in the crystal.[5] Moreover, the NMR spectra of (I) (δ=4.05) at low temperature (Fig. 4) indicate that the methylene proton signals are broadened. It seems that a twisting around the methylene bridges causes the conformers.

The next peak at 26247 cm^{-1} is due to the transition to the $ER_1(-)-CR_1(-)$ state. The band shows regular vibrational progressions at 27624 and 29412 cm^{-1}. The appearance of sharp vibrational progressions indicates that the molecule has a relatively rigid structure. In the following region, several absorption bands were found at 31300, 33800, and 35600—37000 cm^{-1}. The 31300 cm^{-1} band may be due to a transition to the forbidden state of the coupled long-axis transition, $ER_2(+)+CR_2(+)$. The bands at 34000 and 35600 cm^{-1} region are assigned to the CR_2 type bands. The strongest absorption band observed at 38800 cm^{-1} is assigned to the strongly allowed long-axis transition of the coupled dimer, namely to the $ER_2(-)\pm CR_2(-)$ state. It appears from the calculation that two closely situated levels exist in this region.

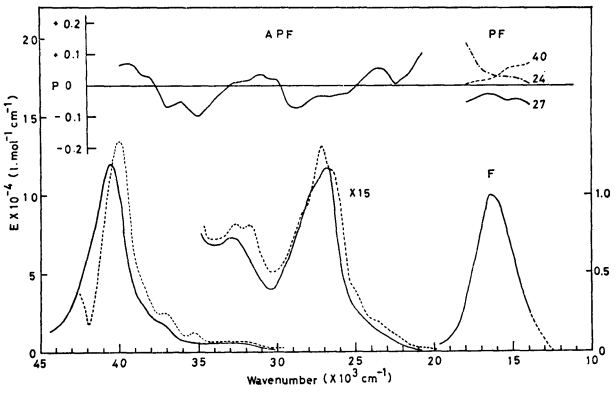

Fig. 5. Absorption spectra of II at 298 K (full line) and at 77 K (broken line) in MTHF with emission spectrum, PF, and APF measured at 77 K. APF monitored at 16000 cm^{-1}.

syn-[*2.2*]*(1,4)Anthracenophane (II).* The absorption spectra measured at room temperature and 77 K are shown in Fig. 5. There are at least seven transitions in the region 20000—45000 cm^{-1}. The lowest band is assigned to a forbidden transition to the $ER_1(+)+CR_1(+)$ state. No absorption related to the excimer emission has been observed in anthracene dimer prepared by photolysis at low temperature. The band can be assigned to the transition to the Franck-Condon state of the excimer level from the ground state. The excimer type fluorescence appears at 16000 cm^{-1}.

Several strong absorption bands were found in the range 24000—29000 cm^{-1} where there are at least three transitions. They are assigned to the coupled $^1B_{3u}$ state (forbidden long-axis polarized band in anthracene, ^1L_b band), $CR_1(-)$ and $ER_1(-)$ bands, respectively. The vibrational progressions are blurred off since the anthracene rings are hinged at the terminal benzene rings and the molecular structure seems to be flexible.

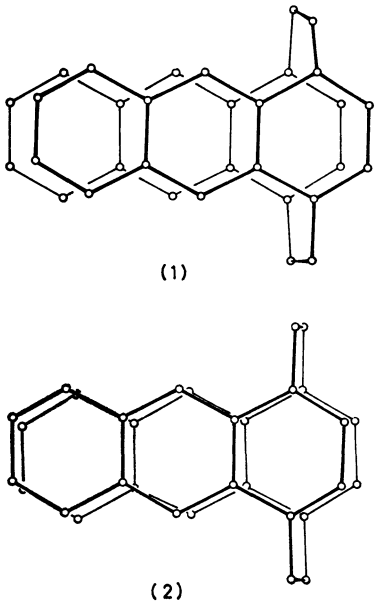

Fig. 6. Molecular structures of II at 124 K.
(1) Slipped form; (2) eclipsed form.

Toyoda and Misumi[5] determined the crystal structure of this molecule at −149 °C and found that two independent molecules are included in a unit cell, taking noticeably different conformations as shown in Fig. 6. One has an approximately symmetric faced conformation, while the other has a displaced or slipped conformation. NMR spectra at low temperature indicate that the methylene protons at $\delta=4$ ppm are broadened in (II) (Fig. 4). This indicates that the methylene bridges are not completely rigid and different conformers may exist at this temperature. The fluorescence spectra of (II) produced by the photocleavage of the photoisomer at 80 K show a peak at 16130 cm^{-1}. It turns into two peaks at 16130 and 16670 cm^{-1} at 140 K and finally is transformed into a single peak centered at 16580 cm^{-1} with enhancement of an intensity of three times. The results also show the presence of conformers at low temperatures.

In the higher energy region several absorption bands were found at 31000—34000, 35000—37000, and 39000—41000 cm^{-1}. The 31000—34000 cm^{-1} band is assigned to the $ER_2(-)-CR_2(-)$ band, which may have long-axis polarization. The band at around 37000 cm^{-1} is calculated to be the mixed higher CR and ER states. The strongest band in the 39000—41000 cm^{-1} region corresponds to the transition to the $ER_2(-)+CR_2(-)$ state.

For assignment of the absorption bands, the analysis of fluorescence polarization spectra would be of most value. The fluorescence spectra were measured at room temperature and 77 K as shown in Fig. 5, the broad excimer type emission band being observed with a peak at 16500 cm^{-1}. The excitation spectra for the red emission are consistent with the absorption spectra of (II), and the excitation efficiency is particularly large at 22000 cm^{-1} where the transition is to the Franck-Condon excimer state of $ER_1(+)+CR_1(+)$. The fluorescence excitation polarization spectra (APF) were measured by observing the fluorescence at 16500 cm^{-1}. The result is shown in Fig. 5 together with the absorption spectra. The first absorption band in the range 21000—22000 cm^{-1} shows the highest positive p value of 0.1. This indicates that the Franck-Condon excited state has nearly the same character as that of the excimer emission, but still the p-value is not high enough to show parallelism of the absorption and emission transition moments. It is very probable that the molecule is deformed in the excited state and the polarization direction of the emission is not exactly the same as of the absorption band. The emissive transition is originally forbidden; it might thus borrow the transition moment from other allowed transitions.

Although the internal molecular motion may occur in the excited state, we can estimate the direction of the transition moment of the emission band based on the p-value of APF for each absorption band at low temperature where the translational molecular motion is frozen. If the excimer state has the strict symmetry of D_{2h}, a radiative transition to the ground state is forbidden, and no emission can be expected. As a matter of fact the fluorescence is observed, hence the symmetry of the excited state should be lowered. However, no polarization study has been published on the excimer state formed by the encounter process in solution. Subudhi, Kanamaru and Lim[19] measured the polarization property on anthracene sandwich dimer and found that the excimer state includes both the short axis component of anthracene $^1B_{2u}(^1L_a)$ type state and the out of plane constituent of CR_1 type state.

In anthracenophanes the emission might appear as a result of the deformation of the molecule in the excited state. Several levels might be mixed to make the transition allowed with a definite polarization direction. The direction might be estimated by correlating the p-value to the long and the short axes polarized transition of anthracene chromophore in anthracenophane. We use the relation of angles between the transition moments of the absorption and the emission:[20]

$$p=\frac{3\cos^2\alpha-1}{3+\cos^2\alpha}, \tag{12}$$

where α is the angle between the emission and the absorption bands.

The direction of the transition moment of the strongest band at 40000 cm^{-1} is certainly along the long-axis; the excimer emission shows positive p-value to the long-axis polarized band. This can occur since the emission state involves the long-axis polarization component. The angle between the transition moment of the emission band and the long-axis is estimated at 48° by Eq. 12. The absorption band in the range 27300—29000 cm^{-1} may have the short-axis polarization (Table 2). The p-value is −0.08 and the angle is found as 60° to the short-axis. The direction of the excimer emission band is thus estimated by using these angles as shown in Fig. 7. In the 26500 cm^{-1} region the p-value is −0.04 and the angle between the absorption and emission transition moments is estimated to be 57° by Eq. 12. The transition of $CR_1(-)$ type may have the polarization in the out of plane direction, and the direction

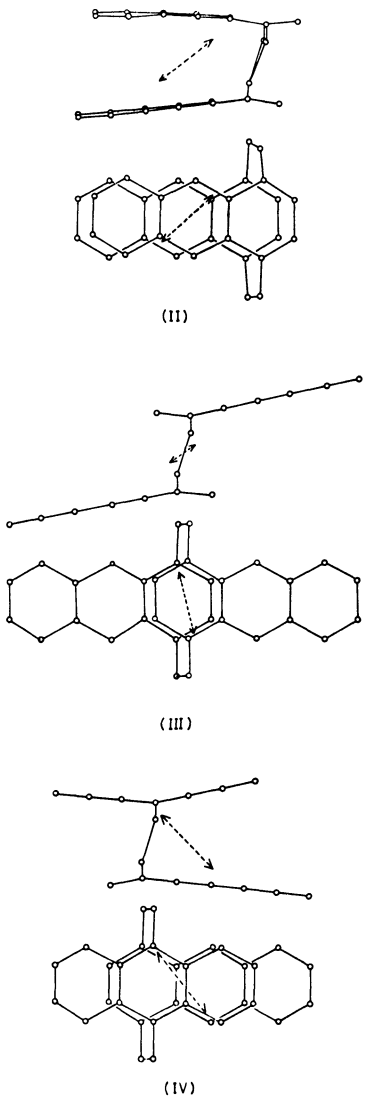

Fig. 7. The directions of the transition moment of emission bands of II, III, and IV estimated from polarization measurements.

makes 56° with the estimated direction of the excimer transition moment. The agreement seems satisfactory.

A positive hump of *p*-value was observed in the 23000—25000 cm^{-1} range, weak shoulders being detected in the absorption spectra. According to theoretical calculation, these weak transitions are attributed to the forbidden transition of the long-axis polarized band originated from anthracene $^1B_{3u}^-$ state (^1L_b type). The 31000 cm^{-1} band shows positive *p*-value, consistent with the assignment of $ER_2(-)+CR_2(-)$, since ER_2 component may have large contribution. In the range 35000—38000 cm^{-1}, the *p*-value is negative. This is reasonable since the transition takes place toward higher CR and the short-axis polarized ER states.

The polarization of the fluorescence band (PF) was measured with excitations fixed at 40000, 27000 and 24000 cm^{-1}, respectively, and the *p*-values were found nearly constant for the 27000 cm^{-1} excitation, varying slightly for the 24000 and 40000 cm^{-1} excitations. This indicates that the excited state involved for the emission band has a mixed character.

The lifetime of the emission was 70 ns, which may be short because of photochemical reaction. It seems that the molecule in the excited state is so deformed that a mixing of an allowed component occurs extensively and both the radiative and the radiationless transitions are enhanced.

anti-*[2.2](1,4)Anthracenophane (III).* The absorption spectra measured at room temperature and 77 K are shown in Fig. 8. The first absorption band consisting of three different bands starts at 23000 cm^{-1} and extends to 31000 cm^{-1}. By lowering the temperature to 77 K, the lowest transition is red-shifted to 23900 cm^{-1}. This is assigned to the $ER_1(+)+CR_1(+)$ state. Several vibrational progressions are observed in the succeeding region. They are classified into two series at 24750, 26180, and 27620 cm^{-1} and 25250, 26740 and 28170 cm^{-1}. Theoretical calculation showed that these are the transitions to the $ER_1(-)\pm CR_1(-)$ states. The splitting of these levels was experimentally estimated as 500 cm^{-1}, while theoretical calculation showed a much larger value. For the molecule with a weak coupling, the present treatment should be modified considering the vibronic effect. The origin of the succeeding band series is not clear and the band at 30000 cm^{-1} is assigned to the higher CR state.

The strongest absorption band is found at 35300 cm^{-1}. This is an allowed long-axis polarized transition which is red-shifted from monomer transition by the exciton type interaction. The red shift as compared to I and II occurred because the arrangement of chromophore is of a head to tail type. The result of calculation shows that two allowed transitions coexist in the 35000—37000 cm^{-1} region, which are regarded to be of $ER_2(-)+CR_2(-)$ type. Another transition was observed at 39500 cm^{-1}, which is ascribed to the long-axis polarized transition of $ER_2(-)-CR_2(-)$.

The fluorescence and the APF spectra measured at 77 K are shown in Fig. 8. The Stokes shift for the

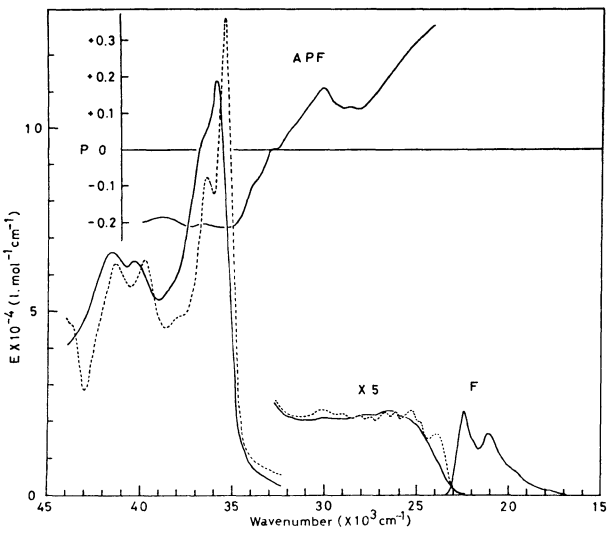

Fig. 8. Absorption spectra of III at 298 K (full line) and at 77 K (broken line) along with emission spectrum and APF at 77 K. APF monitored at 22000 cm^{-1}.

emission is 1500 cm^{-1}, which is smaller than in II and IV but fairly large to indicate the contribution of the CR interaction in the excited state. The APF spectra were measured at 22000 cm^{-1} emission band and the first absorption band at 26000 cm^{-1} shows a high p-value of 0.4. The angle between the emission and the first absorption is estimated to be 23° by Eq. 12, but actually it may be nearly parallel because of inherent experimental error. The bands at 25000—29000 cm^{-1} show positive p-values and the angle is estimated to be about 40°. The two band series are derived from the $ER_1(-)\pm CR_1(-)$ states; the mixing of the CR state with ER state makes the transition moments have an appreciable deviation from the short-axis. In the region of the long-axis polarized transitions, the p-values are all negative, being in line with the assignment of the transitions. The angle between the emission and the long-axis is estimated to be about 71°. By using these angles the direction of the transition moment is estimated as shown in Fig. 7. The lifetime of the emission is 8 ns which is very close to the value of anthracene derivatives. It is consistent with a relatively small shift of the energy level by the dimer type interaction.

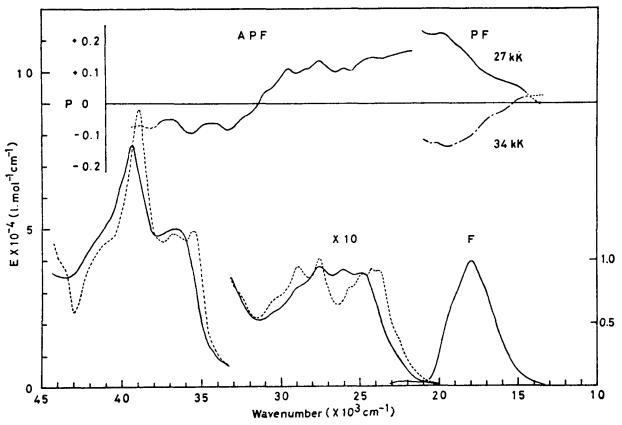

Fig. 9. Absorption spectra of IV at 298 K (full line) and at 77 K (broken line) with emission spectrum, PF, and APF mesured at 77 K. APF monitored at 17500 cm^{-1}.

[2.2](1,4)(9,10)Anthracenophane (IV). The absorption spectra measured at room temperature and 77 K are shown in Fig. 9. The spectra show a conspicuous change at 77 K as compared to that at room temperature, particularly in the lowest energy region. At 22500 cm^{-1} a faint shoulder is observed, but it is not clear whether it is correlated to the lowest calculated level of $ER_1(+)+CR_1(+)$. The strong bands observed at 23800, 24200, 24800, and 25600 cm^{-1} are assigned to the transitions to the $ER_1(-)+CR_1(-)$ state. The succeeding bands found at 27600, 29000, and 30500 cm^{-1} are considered as the transition to the $ER_1(-)-CR_1(-)$ state. The red-shift of the 23800—25600 cm^{-1} bands at low temperature can be explained by a conformational change of the molecule. The NMR spectra (Fig. 4) at low temperature show a broadening of the methylene protons at $\delta=4$ ppm which may be due to the conformational changes. According to a theoretical calculation, a slight change in molecular conformation may cause a significant change in energy levels, therefore a slight change in molecular structure may induce a conspicuous change in absorption spectra. The state which involves the CR configuration will be particularly influenced by a conformational change. The red shift of the 24000 cm^{-1} band can be reasonably understood by a contribution of the CR state to this level.

In the ranges 31500—34000 and 35500—37000 cm^{-1}, the absorption bands detected are ascribed to the $ER_2(-)+CR_2(-)$ state and the higher CR states. The strongest absorption band observed in the 39000—40000 cm^{-1} region is assigned to the $ER_2(-)-CR_2(-)$ state, which is polarized along the long-axis.

The fluorescence and APF spectra measured at room temperature and 77 K are shown in Fig. 9. At low temperature the fluorescence is of a typical excimer type, the Stokes shift being *ca.* 5000 cm^{-1}. APF spectra show positive p-values in the ranges 21500—26000 and 27000—31000 cm^{-1} for the emission band detected at 17500 cm^{-1}.

The results indicate that the polarization of the emission is inclined to the short-axis. In the higher energy region above 32000 cm^{-1}, the p-value is negative. By using Eq. 12 and these p-values, the direction of the transition moment of emission band is estimated as shown in Fig. 7.

The polarization of the fluorescence (PF) is not constant for the whole range of emission bands; the p-value is much more positive in the higher than the lower energy region. A similar result was reported by Subudhi *et al.*[19] for the sandwich dimer formed by the photocleavage of dianthracene in a rigid media. The lifetime of this emission at 77 K is 150—170 ns, typical of the excimer type emission.

Concluding Remarks

The absorption spectra of anthracenophanes show a remarkable change as compared to the sandwich dimer prepared by the photolysis of dianthracene at low temperature. This implies that the inter-ring interaction between anthracene chromophore is much stronger than in the sandwich dimer because the inter-ring distance is shorter than that of normal van der Waals contact. Moreover the planes of the anthracene rings in anthracenophanes are so deformed by ethylene bridges that some fordidden transitions in anthracene appear with lowering in molecular symmetry.

Relative arrangement of the faced rings greatly affects the pattern of the absorption spectra. The charge resonance and exciton type interactions are found to be most important for the interaction between the faced aromatic rings. The absorption bands corresponding to the excimer emission state were observed with weak intensities at the lowest energy region.

The excimer type fluorescence spectra of *syn*-[2.2](1,4)anthracenophane and [2.2](1,4)(9,10)anthracenophane do not differ much from that of the sandwich dimer. A large electron overlap is necessary for the stabilization of the excited state. An overlap of more than two benzene rings is sufficient for the excimer type emission to appear. A large Stokes shift from the

absorption to the fluorescence maximum suggests that the molecules are further deformed in the excited state to cause the stabilization of the excited level and the destabilization of the ground state. The excimer emission state was found to involve nearly a half CR state besides the lowest exciton states of the short- and the long-axis polarization.

References

1) E. A. Chandross, J. Ferguson, and E. G. McRae, *J. Chem. Phys.*, **45**, 3546 (1966).

2) J. Ferguson, A. W.-H. Mau, and J. M. Morris, *Aust. J. Chem.*, **26**, 91 (1973).

3) J. Ferguson and A. W.-H. Mau, *Mol. Phys.*, **27**, 377 (1974).

4) J. Tanaka and M. Shibata, *Bull. Chem. Soc. Jpn.*, **41**, 34 (1968).

5) T. Toyoda and S. Misumi, *Tetrahedron Lett.*, in press.

6) A. Wada and J. Tanaka, *Acta Crystallogr., Sect. B*, **33**, 355 (1977).

7) T. Hayashi, N. Mataga, Y. Sakata, S. Misumi, M. Morita, and J. Tanaka, *J. Am. Chem. Soc.*, **98**, 5910 (1976).

8) J. N. Murrell and J. Tanaka, *Mol. Phys.*, **7**, 363 (1964).

9) T. Azumi, A. T. Armstrong, and S. P. McGlyn, *J. Chem. Phys.*, **41**, 3839 (1964).

10) A. K. Chandra and E. C. Lim, *J. Chem. Phys.*, **48**, 2589 (1968).

11) (a) T. Toyoda, I. Otsubo, T. Otsubo, Y. Sakata, and S. Misumi, *Tetrahedron Lett.*, **1972**, 1731; (b) A. Iwama, T. Toyoda, T. Otsubo, and S. Misumi, *ibid.*, **1973**, 1725; (c) A. Iwama, T. Toyoda, M. Yoshida, T. Otsubo, Y. Sakata, and S. Misumi, *Bull. Chem. Soc. Jpn.*, **51**, 2988 (1978).

12) J. H. Golden, *J. Chem. Soc.*, **1961**, 3741.

13) R. Pariser and R. G. Parr, *J. Chem. Phys.*, **21**, 466 (1953); *ibid.*, **21**, 767 (1953).

14) J. A. Pople, *Trans. Faraday Soc.*, **49**, 1375 (1953).

15) N. Mataga and K. Nishimoto, *Z. Phys. Chem., N.F.*, **13**, 140 (1957).

16) G. Kaupp, *Angew. Chem. Int. Ed. Engl.*, **11**, 313 (1972).

17) J. Ferguson, M. Morita, and M. Puza, *Chem. Phys. Let·.*, **42**, 288 (1976).

18) J. Ferguson, M. Morita, and M. Puza, *Chem. Phys. Lett.*, **49**, 265 (1977).

19) P. C. Subudhi, N. Kanamaru, and E. C. Lim, *Chem. Phys. Lett.*, **32**, 503 (1975).

20) (a) F. Perrin, *Ann. Phys.*, **12**, 169 (1929); (b) A. Jablonski, *Z. Phys.*, **96**, 236 (1935); (c) Th. Förster, "Floreszenz organischer Verbindungen," Vandenhoeck u. Ruprecht, Göttingen (1951).